

EVALUATION OF GAS BUBBLE DURING FOAMY OIL DEPLETION EXPERIMENT USING CT SCANNING

Weifeng LV, Zhenpeng LENG, Xingmin LI, Heping CHEN, Jiru YANG, Ninghong JIA

Research Institute of Petroleum Exploration and Development, Beijing, China

This paper was prepared for presentation at the International Symposium of the Society of Core Analysts held in Snowmass, Colorado, USA, 21-26 August 2016

ABSTRACT

Solution gas drive is an effective way to yield large oil recovery in some heavy oil reservoirs, and it is also identified as foamy oil. Due to the high viscosity of heavy oil that prevents gas bubbles to move, bubbles do not form a continuous gas phase compared with those in conventional oil reservoirs. Although many laboratory investigations and field observations were published around this phenomenon, the mechanism of gas bubble motion remained an essential issue. In this study, a sandpack study is designed to investigate foamy oil displacement mechanism by CT scanning. According to oil and gas production during the entire process, there are 3 stages corresponding to compressibility single oil flow, foamy oil flow and channel gas flow and foamy oil flow accounts for the major recovery. Combining oil saturation images and their histograms, the size and volume of bubbles is determined. Gas bubbles are formed in the foamy oil flow stage, and the quantity of bubbles increases exponentially with depletion pressure decreasing. When it enters into gas channelling flow stage, a continuous gas phase develops. Analyzing oil saturation images of inlet and outlet sections turn out that the low oil saturation regions expand together near the inlet but shows a dispersed distribution at the outlet, which indicates that free gas phase may formed near the inlet and gas bubbles are not connected and foamy oil energy is still effective to enhance oil recovery at the outlet.

INTRODUCTION

Successful heavy-oil reservoir development by solution gas drive has been reported recently. Different from conventional reservoir, heavy oil reservoir with solution gas drive presents unusual development characteristic such as low producing oil-gas ration, high oil recovery rate and more than expected recovery[1]. Studies show some special mechanisms and foamy oil drive is one of them: due to high viscosity of crude oil, gas releases slowly from the liquid phase and starts to flow in relative low gas saturation; at the same time the gas phase mobility doesn't increase with the increasing in saturation. Gas, showing up as tiny bubbles and representing in discontinuous phase, distributes in crude oil and flows in the porous medium. Such dispersed system (e.g. gas bubble surrounded by oil) is called foamy oil and this fluid type is foamy oil fluid[2].

Although the understanding of foamy oil has been deepened in recent years, the flow mechanism of foamy oil in porous medium is still not clear enough[3-6]. Using visual glass micro model can observe the micro-phenomenon and flow mechanism, however,

there is a certain difference between real pores and glass model in temperature and pressure. This study based on real core sample to simulate reservoir pressure and temperature and applies CT scan process to evaluate foamy oil depletion recovery method, focusing on foamy oil production characteristic and establishing a bubble generation evaluating system for bubble quantity, size and other factors.

EXPERIMENTAL

A 45mm (D) ×450mm (L) sandpack filled with 100-120 mesh quartz was used. Its porosity was 36.5% and air permeability was 5541mD, which was similar to the target reservoir. The test live oil was made by CO₂ and CH₄ (mole ratio 13:87), which has a solution gas oil ratio (GOR) of 18.0m³/m³, viscosity of 6151mPa·s, density of 0.98 g/cm³, bubble point pressure (BBP) of 6.07MPa and pseudo bubble point pressure (PBBP) of 4.44MPa at reservoir conditions of 53.7°C.

A GE medical CT scanner is used under 120 kV and 130 mA conditions, and foamy oil analysis software based on CT data was developed by Beijing Digian-Sim Technology Co., Ltd. A set of Quizix pumps was used for fluid injection and backpressure control.

The experimental process can be described as followed: Vacuum the prepared sandpack and saturate it with live oil, and the pressure was maintained at 7.0 MPa during this process. Then close the inlet and step down the backpressure of the outlet. Reduce the pressure by 0.2 MPa each step until the backpressure was stable and no more fluid came out. Terminate the experiment when the outlet pressure reached atmosphere pressure. Maintain the whole system at reservoir temperature, and scan the sandpack and measure the produced oil and gas of every pressure drop.

RESULTS AND DISCUSSIONS

Characteristic of Foamy Oil Depletion

In the initial stage of the experiment, only oil was produced due to the compressibility, where collected gas was escaped from oil at ambient condition. When the pressure dropped slightly lower than the BBP (6.07MPa), oil and gas were produced simultaneously, and a large amount of oil was produced until the pressure reached PBBP (4.44MPa). After that, only a great pressure drop, a little oil can be produced. Meanwhile, bursting gas channelling was shown up intermittently. Accordingly, there were 3 stages corresponding to compressibility single oil flow (Stage I), foamy oil flow (Stage II) and channel gas flow (Stage III).

The production data of oil and gas from experiment were shown as Fig1 (the COP represents cumulative oil production and SOP represents stage oil production, meanwhile, CGP implies cumulative gas production and etc.). It can be seen from Fig 1 that stage I had very limited effect on foamy oil recovery that the accumulated oil production was only 4.8% of the entire experiment. Stage II took the major contribution for the whole system, which occupied 72.3% oil recovery of the entire system. The recovery percent increased rapidly in Stage II after the slow grow in Stage I, but substantially declined in Stage III. It meant that the ultimate recovery, 17.4% in this experiment, relied on the span

of Stage II which determined by the differences between the BBP and the PBBP. Fig 1 (b) showed that the GOR maintained at $18.0\text{m}^3/\text{m}^3$ in Stage I, and slightly rose to $20\sim 35.0\text{m}^3/\text{m}^3$ in Stage II. It can be explained that there were a few dispersed gas in the foamy oil fluid and they acted as discontinued micro bubbles in the oil phase. However, the GOR increased significantly in Stage III, which can reach to $300.0\text{m}^3/\text{m}^3$ and then decline to $60.0\text{m}^3/\text{m}^3$ in the end. The cumulative gas production curve had several increases in this stage, and each change maintained longer than the former one. It indicated that with the increase of degassed oil viscosity, the energy that required for gas bubble to create channel gas flow was also increased. Accordingly, lots of bubbles were trapped in the porous media and channel gas flow was difficult to occur.

Flow Mechanism for Foamy Oil Depletion

In the foamy oil depletion process, the development of gas phase from dissolved gas bubbling out of solution will lead to change of the effective density of the oil / gas-bubble mixture, which is imaged by the medical CT scanner at a resolution of 1 millimeter as an effective phase. CT scanning can monitor the fluid saturation throughout the experiment so to understand the flow mechanism for foamy oil depletion more deeply. Fig 2 and Fig 3 display the oil saturation images and its saturation distribution in each stage.

In Stage I, the total oil saturation was close to 100% but a little lower at the inlet (the blue lines from Fig 2). This may due to the escaped gas with local pressure drop caused by live oil injection. In addition, as this position was far away from the outlet, a huge flow resistant kept these gas stay where they were and lead to a small decline of oil saturation, which meant that small bubbles had been formed near inlet position.

In Stage II, the oil saturation was significantly decreased around BBP (the red cures in Fig 4), which indicated that the optimum production period was the combination of compressibility and foamy oil fluid energy. After that, the oil saturation curves along the sandpack decreased uniformly, which meant that the production effect was proportional to the amplitude of the step- down pressure drop. Comparing the CT images of different positions, it can be seen that the oil saturation showed a uniform decline trend near the outlet, which meant that bubbles were relative small and highly disconnected in this area. While the inlet showed a low oil-saturation zone, which indicated bubbles were generally gathered and grew larger. This phenomenon can be explained that the bubbles formed near the outlet can be produced by foamy oil flow timely, so it is difficult to gather but distributed uniformly. However, the bubbles near the inlet were too far from the end to be produced, so they were trapped by degassed oil with high viscosity and expanded with the pressure drop, and finally gathered into a connected gas phase.

In Stage III, the oil saturation did not decrease obviously with the pressure drop, and the bubbles grew bigger and spread stronger comparing to the previous stage. At the end of this experiment, a connected gas phase was also established near the outlet. After a large number of degassing, the viscosity of oil increased significantly, which lead to the trapping of a large amount of the bubbles. These bubbles expanded and gather into a connected gas phase, even caused bursting gas channelling.

Evaluation of Gas Bubbles in Foamy Oil

In CT scanning, the porosity and saturation of every pixel can be calculated from CT number. Gas bubbles can be identified by setting saturation threshold of pixels considering saturation distribution frequency and images change. This method can be described as followed: When the pressure is lower than BPP, gas will escape and present as unconnected micro-bubbles dispersed in the oil phase. The gas saturation at this moment is called minimal bubble generation gas saturation (MBGGS), accompanied by the sharp decline in the oil saturation distribution frequency (Fig 4). With the pressure continuous decreasing, these micro-bubbles expand and gather. When the pressure is lower than PBBP, the connected gas phase starts to move, and the gas saturation at this moment is called critical gas saturation (CGS). The color of images changes uniformly until CGS, low-oil-saturation zone appears (blue spots on Fig 5), and the distribution frequency of gas saturation that higher than CGS, quite small and even close to zero before, increases rapidly (Fig 4). According to the saturation data of every pixel, gas bubble can be identified and its properties can be analysis by following rules: (1) Gas saturation lower than MBGGS, no bubble; (2) Gas saturation between MBGGS and CGS, discontinuous bubble, and its volume can be calculated by formula (a); (3) Gas saturation higher than CGS, large bubble or continuous gas phase, and its volume can be calculated by formula (b).

$$V_{\text{discontinuous}} = \Delta V_{\text{pixel}} \cdot \Phi_i S_{gi} \quad (a)$$

$$V_{\text{continuous}} = \Delta V_{\text{pixel}} \cdot \sum \Phi_i \cdot S_{gi} \quad (b)$$

V_{single} – discontinuous bubble volume, ml	ΔV_{pixel} – pixel volume, ml
$V_{\text{continuous}}$ – continuous bubble volum, ml	Φ_i – pixel porosity, %
	S_{gi} – pixel gas saturation, %

In this experiment, considering the propagation of the pressure, a CT image slice close to the outlet was analysis. The threshold of MBGGS and CGS were 2.3% and 17.0%, respectively. The volume of discontinuous bubbles was range from 0.00142ml to 0.0141ml, and the volume of continuous bubbles was range from 0.104ml to 12.36ml. Take this slice for example, in Stage II the quantities of bubbles increased exponentially with pressure drop and reached the top of 3592 at PBBP, while these bubbles were all discontinuous. In Stage III the quantities of bubbles showed a little decrease. When the pressure dropped to 4.0MPa, the quantities rose to 3437, but still presented as discontinuous bubbles with a few large bubbles. After that the quantities of bubbles decreased drastically to form large bubbles, and finally there were only 896 bubbles and large bubbles took the main position around 87.4% at ambient condition. In general, the foamy oil stage (Stage II) was the main period for single bubbles to form and the expansion energy of gas perform well displacement of oil, which was the major production period. With a large depletion in pressure, the residual oil has less potential to

produce gas while existing small bubbles gathering into continuous gas phase even to cause gas channelling, which result in reducing oil production.

CONCLUSION

In this study, a foamy oil depletion experiment was conducted to understand the flow mechanism and evaluate the gas bubble by the aid of CT scanning. Some conclusions can be drawn. There were 3 stages in foamy oil depletion process corresponding to compressibility single oil flow, foamy oil flow and channel gas flow. The oil saturation maintained 100% throughout the sandpack in the compressibility single oil flow stage. It was significantly decreased around BBP, which indicated that the optimum production period was the combination of compressibility energy and foamy oil fluid energy, and the foamy oil flow stage accounts for 72.3% accumulated oil recovery of the whole process and the length of this stage directly affects the ultimate oil recovery. In the channel gas flow stage, the isolated gas bubbles expanded and gathered into continuous gas phase even caused bursting gas channelling, which would reduce oil production. The volume of discontinuous bubbles was range from 0.00142ml to 0.0141ml and that of continuous bubbles was 0.104ml to 12.36ml. Bubbles occurred in the foamy oil flow stage and the quantities of discontinuous bubbles increased with the pressure drop. However, when the gas channelling came into being, the quantities of discontinuous bubbles decreased but gather into large bubbles and continuous gas phase, which resulted in reducing oil production.

REFERENCES

1. SHENG,J.J., MAINI, B.B., HAYES, R.E. and TORTIKE, W.S. Critical Review of Foamy Oil Flow, *Transport in Porous Media, Vol.35, p.157-187, 1999.*
2. TANG, G.Q., SAHNI, A., GADELLE, F., KUMAR, M., and KOVSCEK, A.R., Heavy-Oil Solution Gas Drive in Consolidated and Unconsolidated Rock, *SPE 87226, International Thermal Operations and Heavy-Oil Symposium and Western Regional Meeting, Bakersfield, California, 2004.*
3. MAINI, B.B. Effect of Depletion Rate on Performance of Solution Gas Drive in Heavy Oil System, *SPE 81114 presented at the Latin American and Caribbean Petroleum Engineering Conference, Port-of-Spain, Trinidad and Tobago, April 27-300, 2003.*
4. SMITH, G.E., Fluid Flow and Sand Production in Heavy-Oil Reservoirs Under Solution-Gas Drive, *SPE, P169-180, May, 1988.*
5. AKIN, S., and KOVSCEK, A.R., Computed Tomography in Petroleum Research. *Applications of X-ray Computed Tomography in the Geosciences, Geological Society of London, Special Publications, 215, 23-38, 2003.*
6. KOWALEWSKI, E., RENNAN, L., SOLBAKKEN, K., GILJE, E., MELHUUS, K., and RINGEN, J.K., Foamy Oil Experiments Monitored by Computed Tomography Scanning, *World Heavy Oil Congress 2008, Paper 2008-309.*

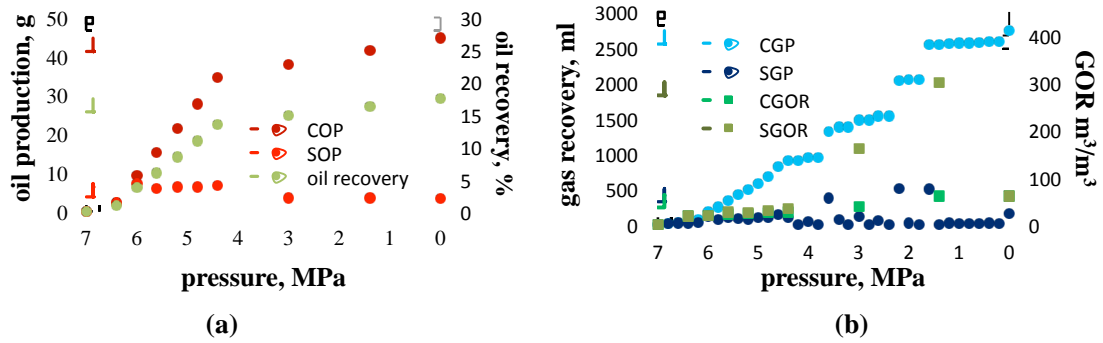


Figure 1. Different Production Parameters with Pressure Change

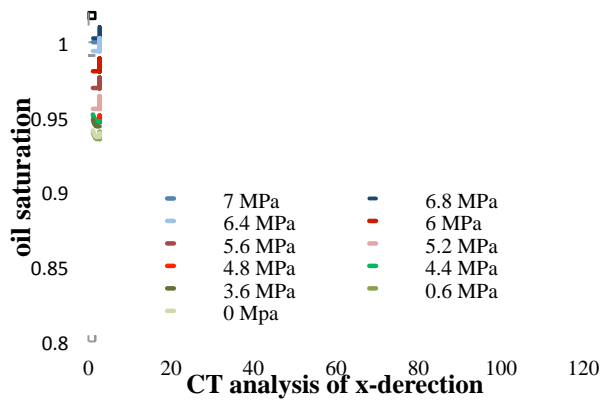


Figure 2. Oil Saturation Changes from Different Stages

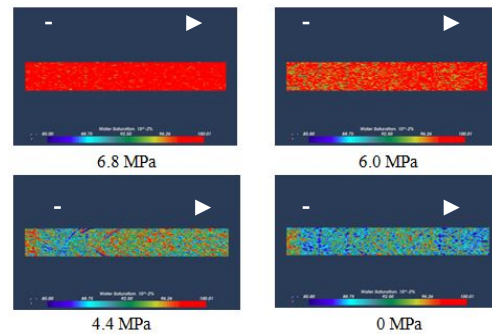


Figure 3. Oil Saturation from CT Images

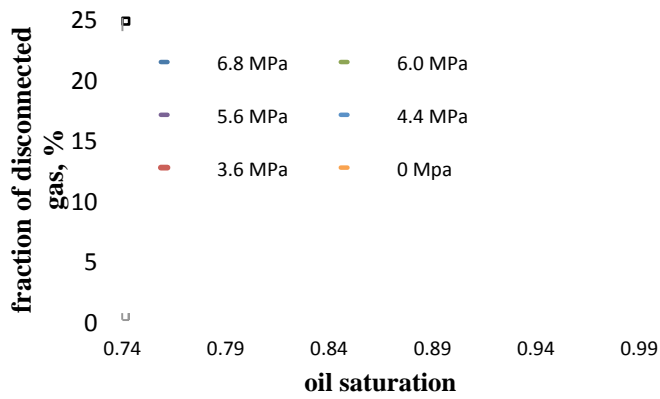


Figure 4. Fraction of disconnected (and immobile) gas v.s. Oil Saturation

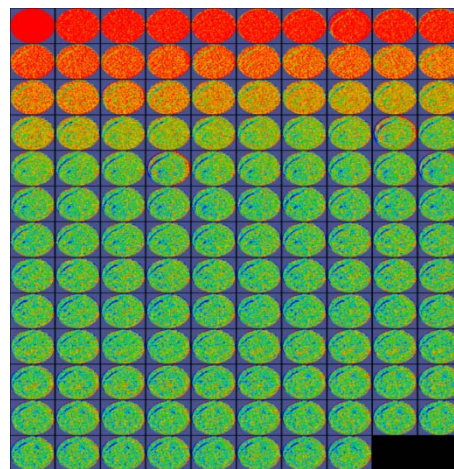


Figure 5. A sample of oil saturation evolution